

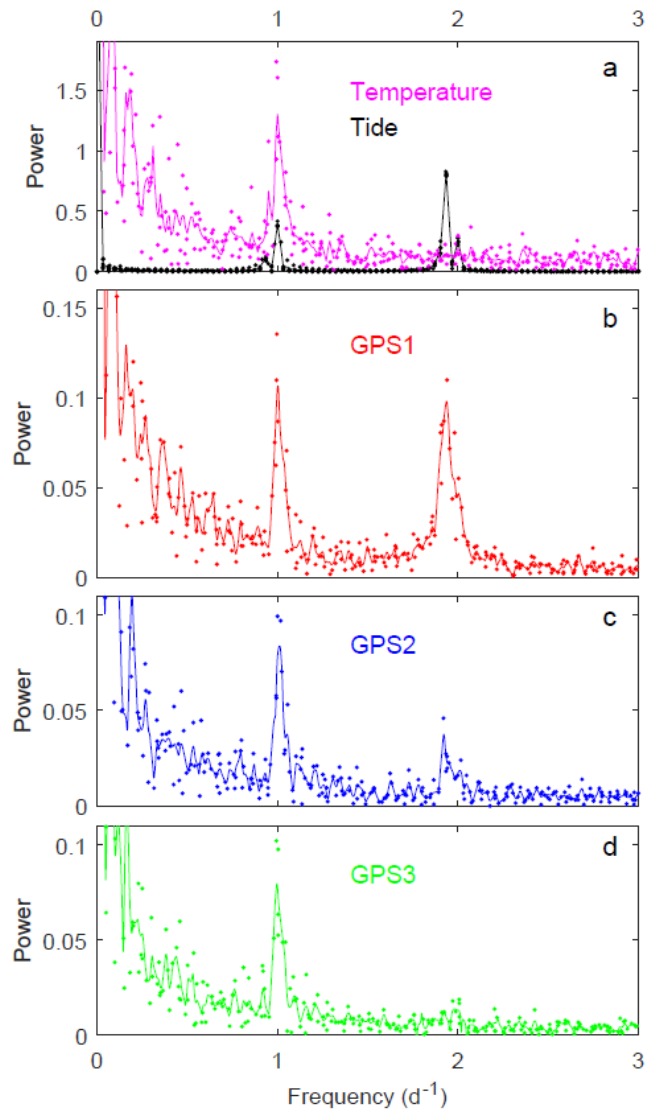
*Supplement of*

**Ice speed of a Greenlandic tidewater glacier modulated by tide, melt, and rain**

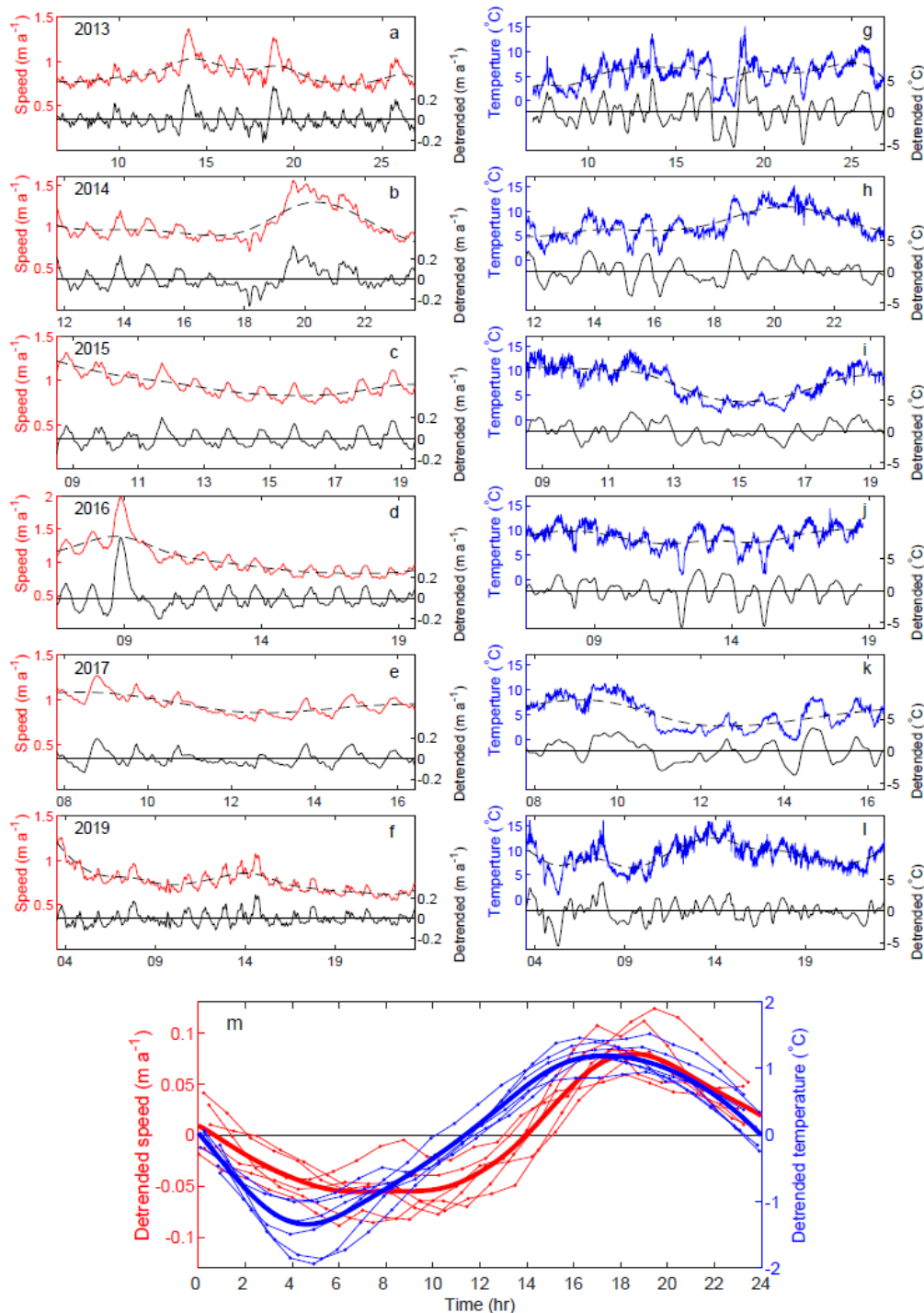
Shin Sugiyama<sup>1,2</sup> Shun Tsutaki<sup>3,4</sup>, Daiki Sakakibara<sup>1,2</sup>, Izumi Asaji<sup>1</sup>, Ken Kondo<sup>1</sup>, Yefan Wang<sup>1</sup>, Evgeny Podolskiy<sup>2</sup>, Guillaume Jouvét<sup>5,6</sup> and Martin Funk<sup>6</sup>

- 5 <sup>1</sup> Institute of Low Temperature Science, Hokkaido University, Sapporo, Japan  
<sup>2</sup> Arctic Research Center, Hokkaido University, Sapporo, Japan  
<sup>3</sup> National Institute of Polar Research, Tokyo, Japan  
<sup>4</sup> Department of Polar Science, The Graduate University of Advanced Studies, Tokyo, Japan  
10 <sup>5</sup> Institute of Earth Surface Dynamics, University of Lausanne, Lausanne, Switzerland  
<sup>6</sup> Laboratory of Hydraulics, Hydrology and Glaciology, ETH Zurich, Zurich, Switzerland

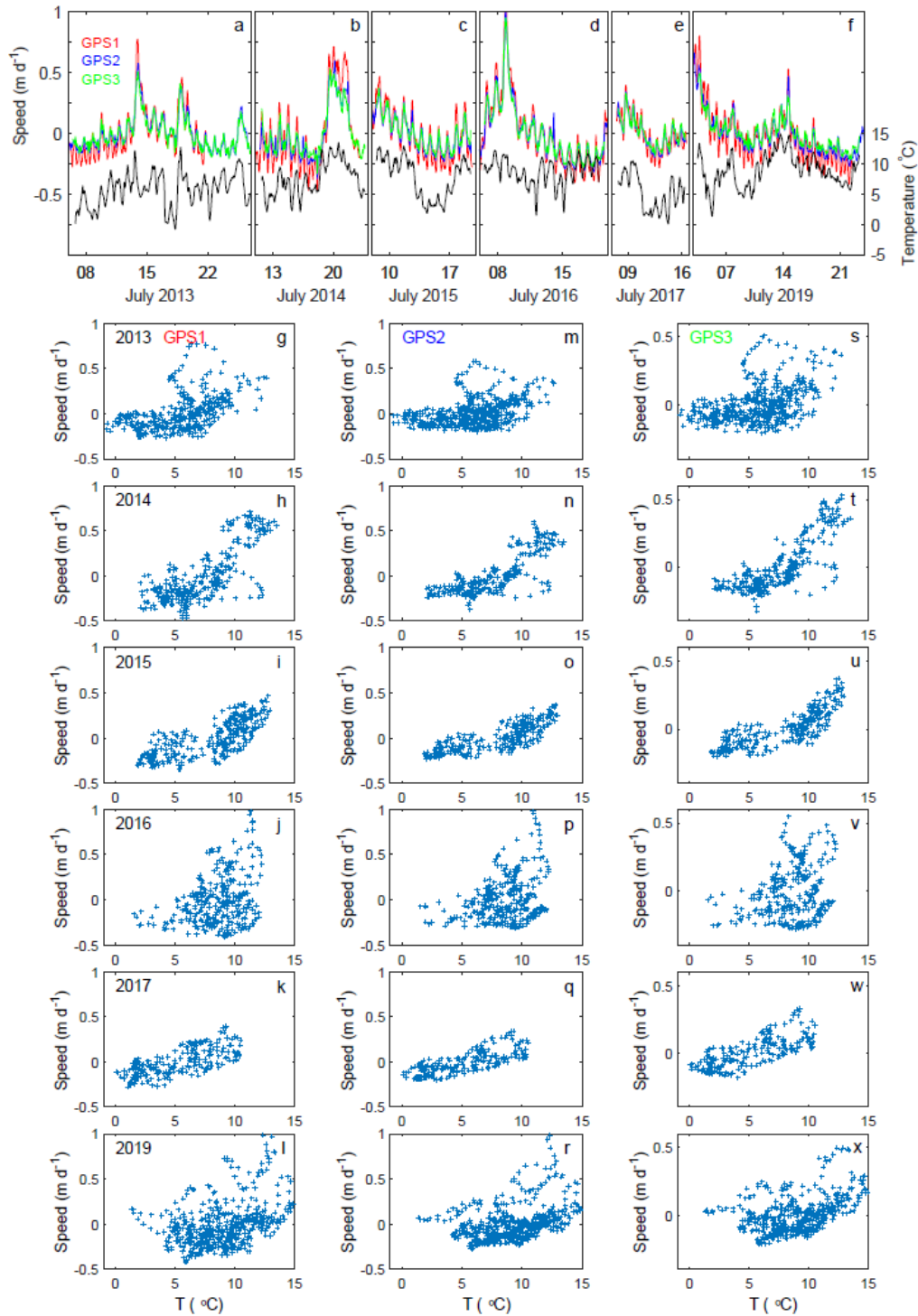
*Correspondence to:* Shin Sugiyama (sugishin@lowtem.hokudai.ac.jp)



15 **Figure S1.** Frequency analysis of air temperature, tide, and ice speed. Power spectral diagrams for (a) air temperature (magenta) and tide (black), (b) ice speed at GPS1, (c) ice speed at GPS2, and (d) ice speed at GPS3. Solid curves were obtained by filtering power (dots) computed by Fourier transformation of the data for 2013–2017 and 2019.



20 **Figure S2.** Diurnal pattern analysis of ice speed and air temperature. (a–f) Ice speeds at GPS3 in July 2013–2017 and 2019. Detrended speed (solid black line) was obtained by subtracting a trend (dashed black line) from the data (red). (g–l) Same as (a–f) but for air temperature. (m) Diurnal variations in the detrended ice speed (red) and temperature (blue). Each curve was obtained by connecting values averaged in each year. The thick curves are the mean of the six years.



25 **Figure S3. Ice speed and air temperature variations. (a–f) Detrended ice speed at GPS1–3 (red, blue, and green) and air temperature. (g–x) Scatter plots of air temperature and detrended hourly mean ice speed at (g–l) GPS1, (m–r) GPS2, and (s–x) GPS3.**

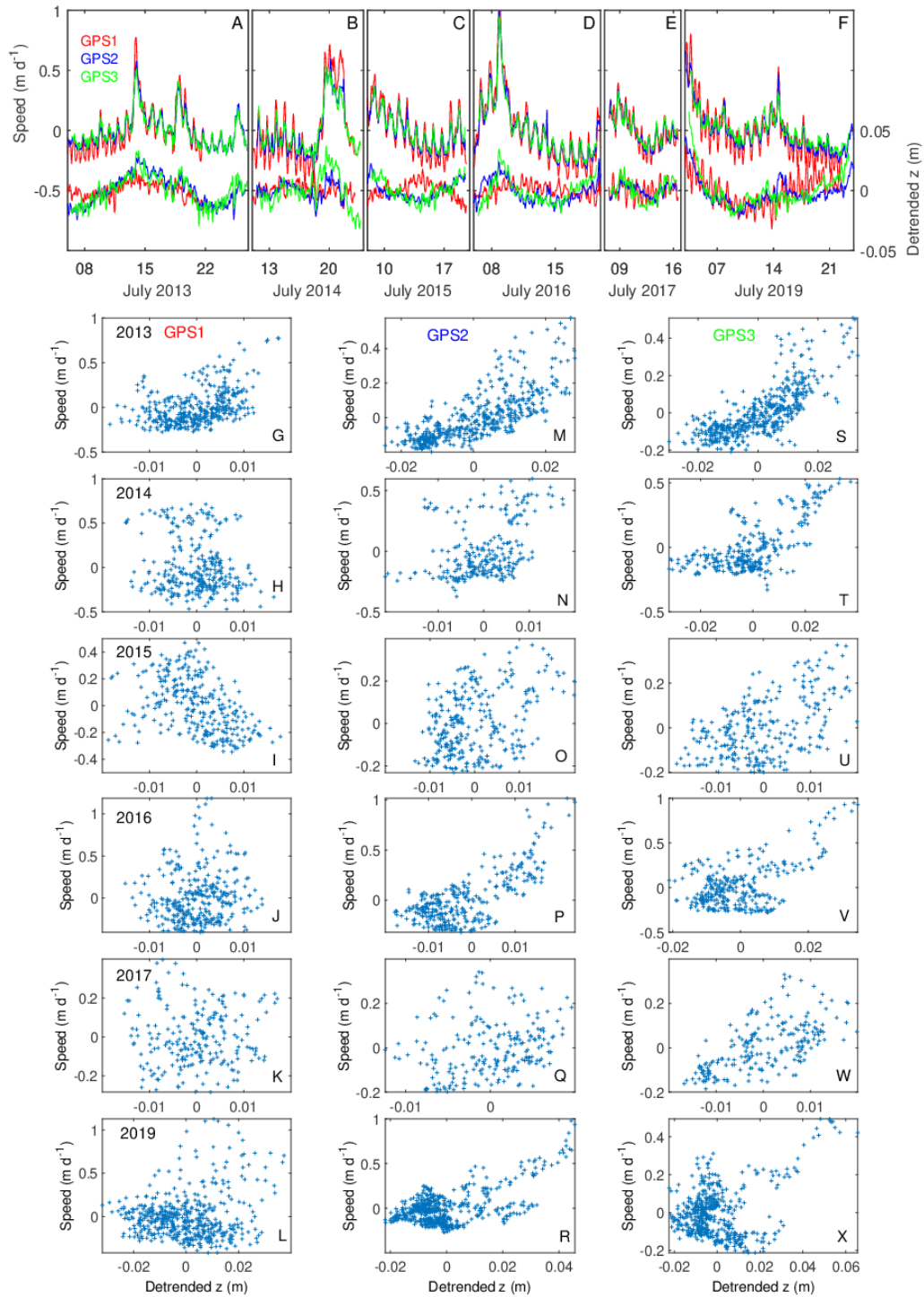


**Figure S4. Ice speed variations and glacier surface uplift. (a–f) (top) Detrended ice speed and (bottom) vertical coordinate at GPS1–3 (red, blue, and green). (g–i) Scatter plots of detrended hourly mean ice speed and the vertical coordinate at (g–l) GPS1, (m–r) GPS2, and (s–x) GPS3. Note that the x- and y-axis scales are different in each panel.**